Finite Element Modeling of Crustal Deformation in the North America–Caribbean Plate Boundary Zone

P. R. Lundgren[1] and R. M. Russo[2,3]

[1]*Jet Propulsion Laboratory*
California Institute of Technology
4800 Oak grove Drive, MS 183-S01
Pasadena, CA 91109-8099
Phone: (818) 354-179S; IAX: (818) 393-.$0S9.

[2]*Department of Terrestrial Magnetism*
Carnegie Institution of

[3]*Now at: Laboratoire de Tectonophysique*
Université Montpellier II
Place Eugene Bataillon
34095 Montpellier Cedex 05, France

Finite Element Modeling of Crustal Deformation in the North America- Caribbean Plate Boundary Zone

P. R. Lundgren[1] and R. M. Russo[2,3]

[1]*Jet Propulsion Laboratory*
California Institute of Technology
4800 *Oak grove Drive., MS 183-S01*
Pasadena, CA 9110W1099
Phone: (818) 354-1795; FAX: (818) 393-3059.

[2]*Department of Terrestrial Magnetism*
Carnegie Institution of Washington
5241 Broad Branch Road, N. W.
Washington, DC 20015

[3]*Now at: Laboratoire de Tectonophysique*
Université Montpellier II
Place Eugene Bataillon

velocity closure requirements predict only 1 ? mm/yr NA-Ca relative motion al [he. Cayman sprinting axis. *Deng and Sykes [1995]* used a least squares method to compute an NA-Ca Euler pole from NA-Ca PBZ earthquake slip vectors and then calculated an angular rotation rate such that it produces 20 mm/yr relative motion al the Cayman spreading center. They proposed that the mean rate derived from Cayman Trough spreading underestimates the full plate motion because of past or current slip along presumed Cayman fracture zones, and that motion directions based on Cayman transform faults may be unreliable if deformation has modified their azimuths [*Sykes et* al., 1982]. Thus, NUVEL-1 accounts for no distributed deformation in the.

Mann et al., 1991]. Seismicity along the fault (Figure 2) clearly indicates pure left-lateral slip. We infer from the simplicity of Swan Islands Fault structures and seismicity that the fault is the plate boundary and that motion here is not distributed across a wide zone as it is further east. The Swan Islands Fault terminates eastward at the southern end of the Cayman spreading center, which has normal faulting earthquakes (Figure *2)* and generates the magnetic anomalies of the Cayman Trough [*Rosencrantz et* al., 1988]. The northern end of the Cayman spreading ax is

underthrusting of Caribbean lithosphere beneath terranes including eastern Hispaniola and Puerto Rico [*Byrne et 01., 1985; A4cC."arm and Pennington,* 1990; *Masson and Scanlon 1991],* South of Puerto Rico there is evidence that Muertos Trough convergence decreases eastwards [*Masson and Scanlon,* 1991] with strike-slip motion [P. Jansma, *personal communication, 1995]* near its intersection with the

where in the finite element array. A Monte Carlo technique is used to interpret the sensitivity and uncertainties in the model due to complexities in the data. For our application to [he northern Caribbean region, wc solve for nodal displacements on an elastic, 2-D spherical shell with a plane stress condition (σ_3 = O). We usc eight node, biquadratic, isoparametric elements.

The crustal layer is modeled as a two dimensional elastic plate, cut by active fauns. Faults arc surfaces in which 1) only the slip direction is constrained; *2)* both the slip direction and rate are known; or 3) both the direction and rate are unconstrained. Fault slip data arc implemented as described by *Melosh and Raefsky [1981],* and introduce torque-free dislocations in the continuum. Fault orientations arc prescribed as fi cc-shear surfaces [*Melosh and Williams*, 1 *'989].*

Far field displacements arc imposed as boundary conditions. For a spherical geometry, relative plate motions imposed at the mesh boundary are calculated based on a give.rl boundary node's angular distance from the Euler pole. I,ikc.wise, the overall orientation of the finite element mesh boundaries arc controlled by the Euler pole location since we choose to have the boundaries fail on either great or small circles relative to the rotation pole. q'bus, when wc compare models based on different poles, the locations of the mesh boundaries reflect differences in pole location.

The most significant difference between this approach and the rigid

on a spherical shell is:

$$\varepsilon = \begin{bmatrix} \varepsilon_\theta \\ \varepsilon_\phi \\ 2\varepsilon_{\theta\phi} \end{bmatrix} = \frac{1}{R}\left\{ \begin{bmatrix} \frac{\partial}{\partial\theta} & 0 \\ 0 & \frac{1}{\sin\theta}\frac{\partial}{\partial\phi} \\ \frac{1}{\sin\theta}\frac{\partial}{\partial\phi} & \frac{\partial}{\partial\theta} \end{bmatrix} + \begin{bmatrix} 0 & 0 \\ \cot\theta & 0 \\ 0 & -\cot\theta \end{bmatrix} \right\} \begin{bmatrix} u_\theta \\ u_\phi \end{bmatrix} = Su = SN\zeta = B\zeta \qquad (2)$$

where. (θ, ϕ) arc the. colatitude and longitude, respectively, and R is the radius of the shell (radius of the earth). For an elastic body in equilibrium, we use a variational principle to solve for the minimum in the pole.nlial energy with respect to small nodal displacements. } 'or a given element, e, the elastic strain energy is

$$U^e = \frac{1}{2}\int_{\Omega^e} \varepsilon^T \sigma \, d\Omega \qquad (3)$$

and using Hooke's law (1),

$$U^e = \frac{1}{2}\int_{\Omega^e} \varepsilon^T D\varepsilon \, d\Omega = \frac{1}{2}\int_{\Omega^e} \zeta^{e\,T} B^{e\,T} D^e B^e \zeta^e \, d\Omega \qquad (4)$$

where Ω^e is the element volume. For a boundary traction vector t applied on the boundary of the element, the potential energy of the applied boundary stress is

$$U^e = -\int_S u^T t \, (ls = \int_S \left[N\zeta^{e} \right]^T t \, (ls \qquad (5)$$

where S is the surface of the element. Summing (4) and (5) and minimizing the total energy of the body under load with respect 10 small variations in ζ_i, we get the standard finite element equation:

$$K\zeta = f \qquad (6)$$

where

$$K^e = \int_{\Omega^e} B^{e\,T} D^e B^e \, d\Omega \qquad (7)$$

(ic.fines the element stiffness matrix and

$$f^e = \int_S N^{e\,T} \, dS \qquad (8)$$

defines the element force vector. The global stiffness matrix K is assembled from K^e and is solved for by Gaussian integration. Displacement boundary conditions and fault slip data (split nodes) enter into (8) which reduces the rank to the number of degrees of freedom. A sufficient condition for K to be inverted is that the translation and rotation for each element are constrained so the solution $\zeta = K\text{-}if$

exists.

We calculate uncertainties in the model predictions via a Monte Carlo method to construct the probability distribution for the deformation everywhere. This is computationally efficient since the kinematic data enter the model in the force vector f, so the stiffness matrix, K, is inverted only once. Histograms are constructed from typically

Discussion

The NUVEL-1-based model (where mesh orientation and far-field boundary rates are based On the NUVEL-1 model of *DeMets et al.*, 1990; see Figure 3) is the only model which clearly does not fit the observed left-lateral motion along the Walton-Plantain Garden-Enriquillo fault system [*Mann et al., 1995] and* the observed compression at the Jamaica restraining bend [*Burke et al.*, 1980; Fig. 2 focal mechanism]. This is not unexpected given that its far field NA-Ca rate is less than the observed Cayman spreading rate. Despite this, we note how similar the NUVEL-1 derived motion patterns are in the eastern

Septentrional to the eastern Enriquillo fault, in central Hispaniola gives slow thrust motion from 1-4 mm/yr along its length, consistent with field observations [*Mann et al., 1* 995].

The C&M and D&S models differ most significantly in the easternmost PBZ between Puerto Rico and the Anegada Passage fault system. Morphology, bathymetry, and seismicity indicate that the Anegada Passage fault system is an actively extending graben [*Murphy and McCann, 1979; Frankel et al.,* 1980; *Jany et al., 1990; Masson and Scanlon,* 1991; *Speed and Larue,* 1991]. The Anegada Passage extension direction is no[well constrained by earthquake focal mechanisms,

right-lateral component along the fault sys(<'in has beer) proposed

GPS site FRAN has ESE directed motion. If we in~it[]w.pure strike-sli~) motion 011 the central portion Of the Septentrional fault, W C find a solution (Figure 8) in which the crustal motion at FRAN is ESE-directed, and a normal component of motion is transferred to the fault system off the NE coast of Hispaniola. This result indicates that there is both vertical and horizontal strain partitioning in the restraining bend here: the thrust motions observed by *Russo and Villaseñor* [1995] (see Fig. *2)* occur on a deeper crustal fault or faults beneath NE Hispaniola, and the surficial

cate that NA-Ca relative motion is partitioned as displacement along faults and as continuum deformation (including rotation) throughout the NA-Ca plate boundary zone. Our results are in good agreement with preliminary GPS results [*Farina et al.*, 1995], if we constrain the central Septentrional fault to left-lateral strike-slip motion.

Acknowledgements

We thank Pam Jansma for generously sending us unpublished data and for helpful discussion. Bob Speed read and helped correct flaws in an early version of this work. We thank Eric Calais, Chuck DeMets, and Paul Mann, for critical reviews of the manuscript. Bill McCann offered useful advice. We thank Guilhem Barruol for use of computer facilities and logistical help. A research associateship at the Department of Terrestrial Magnetism and NSF Grant EAR 93-16-1 S") to P. Silver and R. Russo supported R. Russo during this work. Support for P. Lundgren was provided by the Jet Propulsion Laboratory, California Institute of Technology, under contract to the National Aeronautics and Space Administration.

References

Burke, K., J. Grippi, and A. M. C. Şengör, Neogene structures in Jamaica and the tectonic style of the northern Caribbean plate boundary zone, *J. Geol.*, *88*, 375-386, 1980.

Byrne, D. B., G. Suarez, and W. R. McCann, Muertos Trough subduction - microplate tectonics in the northern Caribbean?, *Nature*, *317*, 420-421, 1985.

Calais, E., and B. Mercier de Lépinay, From transtension to transpression along the northern Caribbean plate boundary off Cuba: Implications for the recent motion of the Caribbean plate, *Tectonophys.*, *16'6 ,329-350,* 1991.

Calais, E., and B. Mercier de Lépinay, Semiquantitative modeling of strain and kinematics along the Caribbean/North America strike-slip plate boundary zone, *J. Geophys. Res.*, *98*, 8293-8308, 1993.

Chase, C.G., The *n*-plate problem of plate tectonics, *Geophys. J.R. Astr. Soc.*, *29*, 117-122, 1972.

DeMets, C., R. G. Gordon, D.F. Argus, and S. Stein, Current Plate Motions, *Geophys. J. Int.*, *101*, 425-478, 1990.

Deng, J., and L. R. Sykes, Determination of Euler pole for contemporary relative motion of Caribbean and North American plates using slip vectors of interplate earthquakes, *Tectonics*, 14, 39-53, 1995.

Dillon, W. P., J. A. Austin, K. M. Scanlon, N. T. Edgar, and L. M. Parson, Accretionary margin of north-western Hispaniola: morphology, structure and development of the northern Caribbean plate boundary, *Mar. Pet. Geol.*, *9*, 70-88, 1992.

Dziewonski, A. M., "J'. -A. Chou, and J. H. Woodhouse, Determination of earthquake source parameters from waveform data for studies of global and regional seismicity, *J. Geophys. Res.*, *86*, 2825 -2852, 1981.

Farina, F., E. Calais, C.

Ladd, J. W., T. C. Shih, and C. J. Tsai, Cenozoic tectonics of central Hispaniola and adjacent Caribbean Sea, *Am, Assoc. Petrol. Geol. Bull., 65*, 466 489. *1981.*

Langer, C. J., and G. A. Bollinger, Secondary faulting near the terminus of a seismogenic strike-slip fault: aftershocks of the 1976 Guatemala earthquake, *Seism. Soc. Am. Bull., 69*, 4?.7-444, 1979.

Lundgren, P., F. Saucier, R. Palmer, and M. Langon Alaska crustal deformation: Finite element modeling constrained by geologic and VLBI data, J. *Geophys. Res., irr press*, 1995.

Mann, P., K. Burke, and T. Matumoto, Neotectonics of Hispaniola: plate motion, sedimentation, and seismicity at a restraining bend, *Earth Planet. Sci. Lett*, 70, 31 1-324, 1984.

Mann, P., F. W. Taylor, R. L. Edwards, and T.-L. Ku, Actively evolving microplate formation by oblique collision and sideways motion along strike-slip faults: An example from the northeastern Caribbean plate margin, *Tectonophysics*, in press, 1995.

Mann, P., S. A. Tyburski, and E. Rosencrantz, Neogene development of the Swan Islands restraining-bend complex, Caribbean Sea, *Geology, 19*, 823- 8?6, 1991,

Masson, D. G., and Stanton, K. M., The neotectonic setting of Puerto Rico, *Geol. Soc.* Am. *Bull., 103*, 144-154, 1991.

McCann, W. R. and W. D. Pennington, Seismicity, large earthquakes, and the margin of the Caribbean plate, in *The* Geology *of North America, vol. H, The Caribbean Region*, pp. 291- *306,* edited by G. Dengo and J. E. Case, Geol. Sot. Am., Boulder, 1990.

Melosh, H. J., and A. Raefsky, A simple and efficient method for introducing faults into finite element computations, *Seism. Sot. Am. Bull., 71*, 1391-1400, 1981.

Melosh, H. J., and D. R, Williams, Mechanics of graben formation in crustal rocks: a finite element analysis,.]. *Geophys. Res.*, %', 13,961-13,9?2, 1989.

Minster, B.J., and T.H. Jordan, Present-day plate motions, *J. Geophys. Res., 83*, 53 31-5354, 1978.

Molnar, P., Gravity anomalies and the origin of the Puerto Rico Trench, *Geophys. J. R. A. S., 51*, 701-708, 1977.

Molnar, P., and L. R. Sykes, Tectonics of the Caribbean and Middle America regions from focal mechanisms and seismicity, *Geol. Soc. Am. Bull., 80*, 1639-1684, 1969.

Murphy, A, J., and W. R. McCann, Preliminary results from a new seismic network in the northeastern Caribbean, *Seism. Soc. Am. Bull., 69*, 1497.1513, 1979.

Prentice, C. S., P. Mann, F. W. Taylor, G. Burr, and S. Valastro, Paleoseismicity of the North America-Caribbean plate boundary (Septentrional fault), Dominican Republic, *Geology*, 21, 49-42, 1993

Reid, J. A., P. W. Plumley, and J. }1. Schellekens, Paleamagnetic evidence for Late Miocene counter-clockwise rotation of north coast carbonate sequence, Puerto Rico, *Geophys. Res. Lett., 18,* 565-568, 1991.

Rosencrantz, E., and P. Mann, SeaM ARC II mapping of transform faults in the Cayman Trough, Caribbean Sea, *Geology, 19*, 690-693, 1991.

Rosencrantz, E., M. 1. Ross, and J. G. Sclater, Age and spreading history of the Cayman trough as determined from depth, heat flow, and magnetic anomalies, *J. Geophys. Res., 93*, ?,141–2,157, 1988.

Russo, R. M., and A. Villaseñor, The 1946 Hispaniola earthquakes and the tectonics of the Nor-lb America-Caribbean plate boundary zone, northeastern Hispaniola, *J. Geophys. Res., in press*, 1995.

Saucier, F., and E. Humphreys, Horizontal crustal deformation in southern California from joint models of geologic and very long baseline interferometry measurements, in *Contributions of Space Geodesy to Geodynamics: Crustal Dynamics*, Geodynamics ? 3, edited by D. E. Smith and D. 1.. Turcotte, 139-176.1993.

Speed, R. C. and D. K, Larue, Extension and transtension in the plate boundary zone of the northeastern Caribbean, *Geophys. Res. Lett., 18*, 573-5'/6, 1991.

Stein, S., J. Engeln, D. Wiens, K. Fujita, and R. Speed, Subduction seismicity and tectonics in the Lesser Antilles Arc, *J. Geophys. Res., 87*, 8642-8664, 1982.

Stein, S., C. DeMets, R. G. Gordon, J. Brodholt, D. Argus, J. F. Engeln, P. Lundgren, C. Stein, D. A. Wiens, and D. F. Woods, A test of alternative Caribbean plate relative motion models, *J. Geophys. Res.,*

Tomblin, J. F., The Lesser Antilles and Aves Ridge, in *Ocean Basins and Margins*, Vol. 3, edited by A. E. M. Nairn and F. G. Stehli, pp. 467-500, Plenum, New York,

Zienkiewicz, O. C. and R. L. Taylor, The finite

Figure 4b. *Deng and Sykes [1995]* based model: fault rate solution (see Figure 3b for explanation).

Figure 5a. *Calais and Mercier a'r Lépinay* [1993] based model: calculated motions at the center of each element (se-c Figure 3a **for** explanation)

Figure 5b. *Calais and Mercier de Lépinay* [1993 based model: fault rate solution (see Figure 3b for explanation).

Figure 6. Preliminary GPS site velocity vectors arid their 95% confidence ellipses with respect to site TURK in the Bahamas on stable North America plate for two occupations in 1986 and 1994 from *Farina et al. [1995].*

Figure 7 *Calais* **and** *Mercier de Lépinay [* 1993] based model (inset of Puerto Rico area): calculated motions at the center of each element (see Figure 3a for explanation). This is the same solution as Figure 5a but with the North America plate held fixed so that the continuum velocity vectors can be compared to Figure 6.

Figure 8 *Calais and Mercier de Lépinay* [*1993]* based model (inset of Puerto Rico area): (a) calculated motions at the center of each element (see Figure 3a for explanation). This is the same as Figure 7 but with the added constraint that the central Septentrional fault be strike-slip. This produces continuum motions mom consistent with the GPS results shown in Figure 6. (b) fault rate solution (see Figure 3b for explanation).

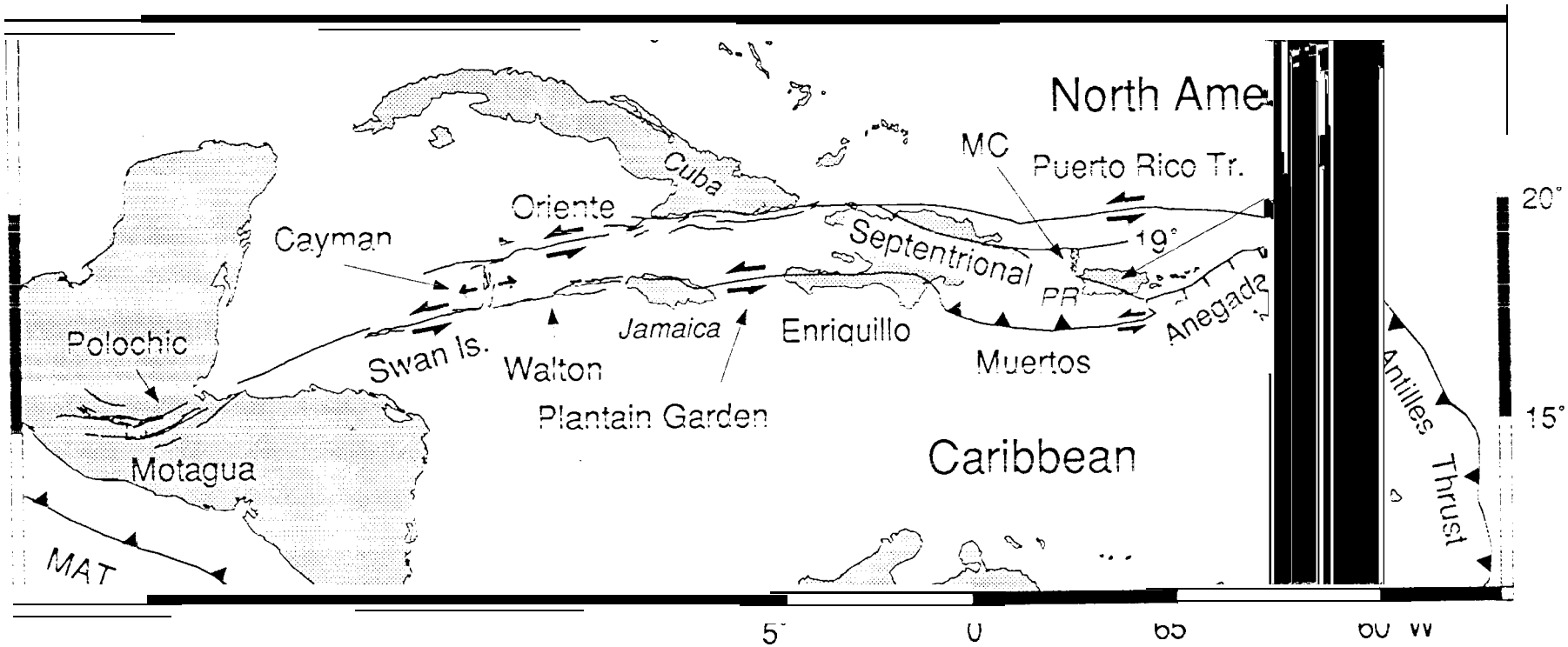
North Ame
MC
Puerto Rico Tr.
Cuba
Oriente
Cayman
Septentrional
19°
PR
Anegada
Polochic
Swan Is.
Walton
Jamaica
Enriquillo
Muertos
Plantain Garden
Caribbean
Motagua
MAT
Antilles
Thrust
20°
15°
5°
0
65
60 W

Figure

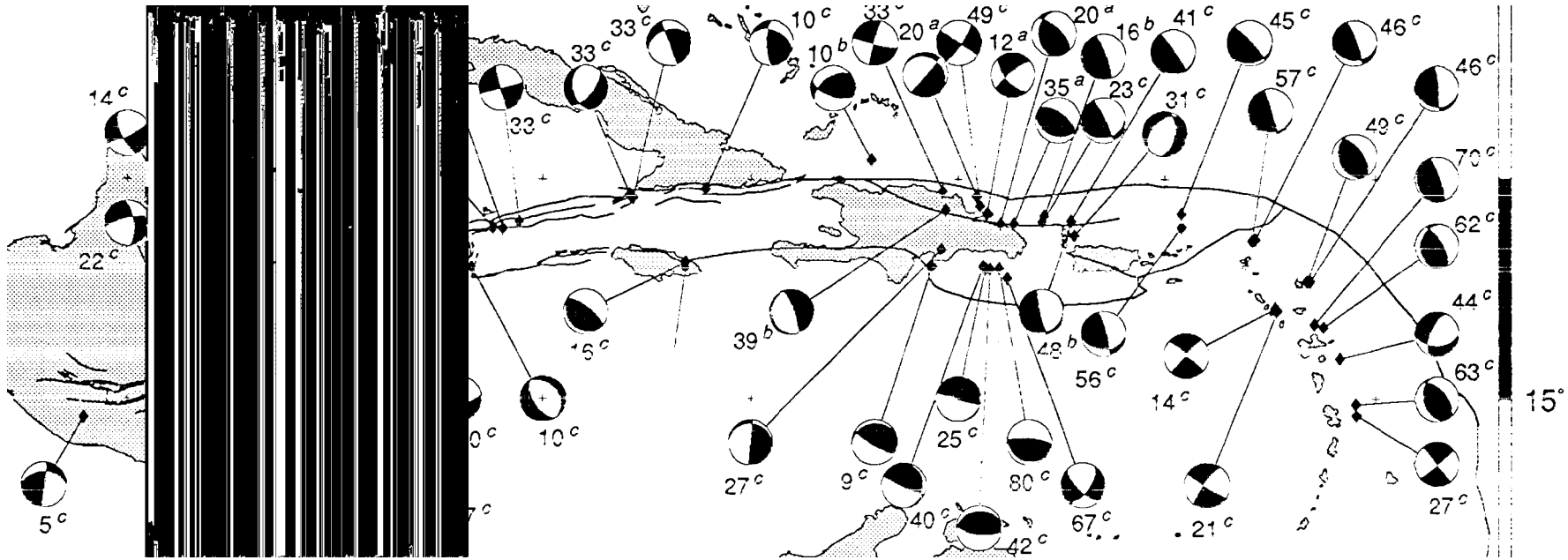
14c
22c
5c
33c
33c
33c
10c
10b
20a
49c
12a
20a
16b
41c
45c
46c
35a
23c
31c
57c
46c
49c
70c
62c
44c
63c
27c
39b
48b
56c
14c
25c
27c
9c
40c
80c
67c
42c
21c
10c
15°

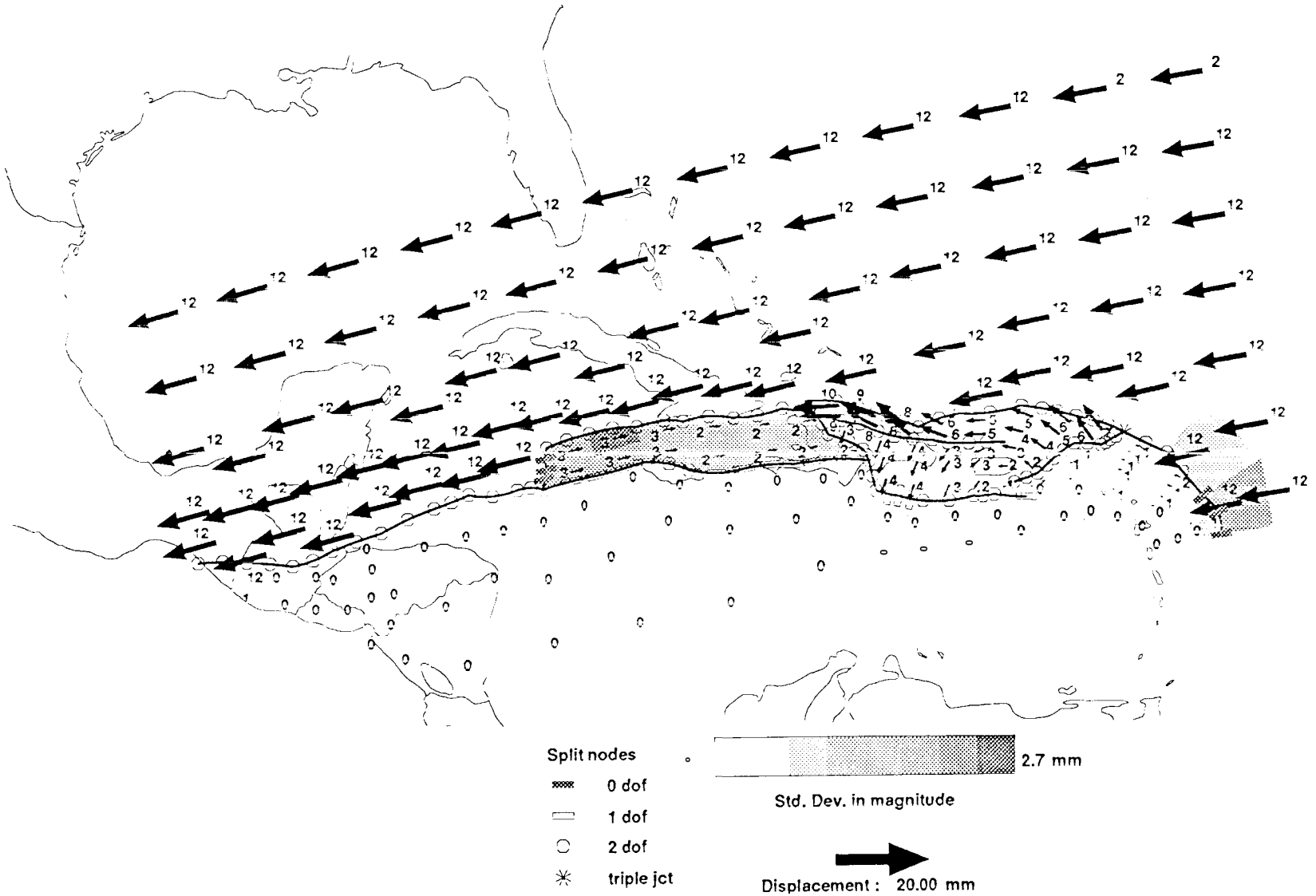
Split nodes
0 dof
1 dof
2 dof
triple jct
2.7 mm
Std. Dev. in magnitude
Displacement : 20.00 mm

Figure 3a

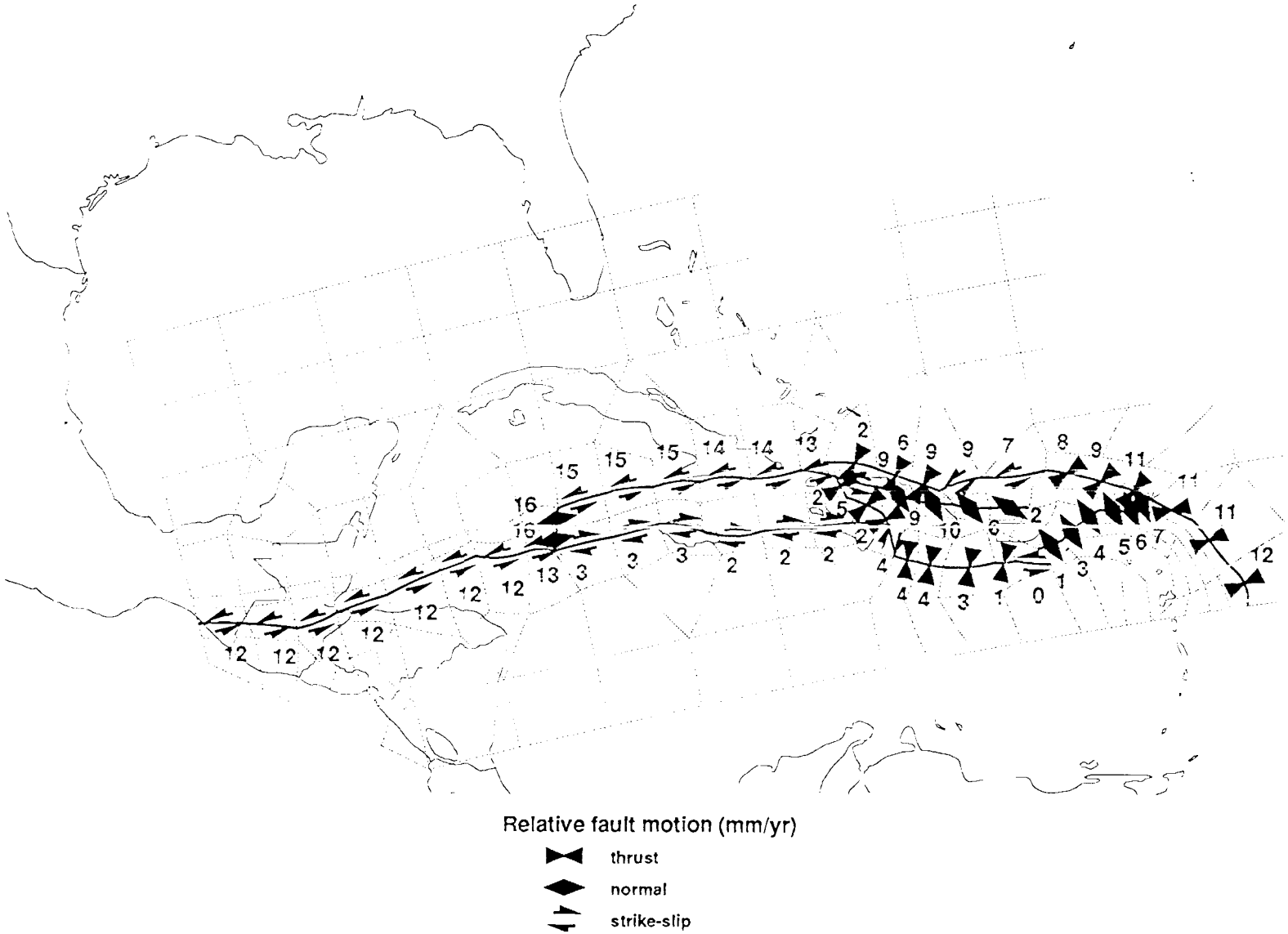

Figure 3b

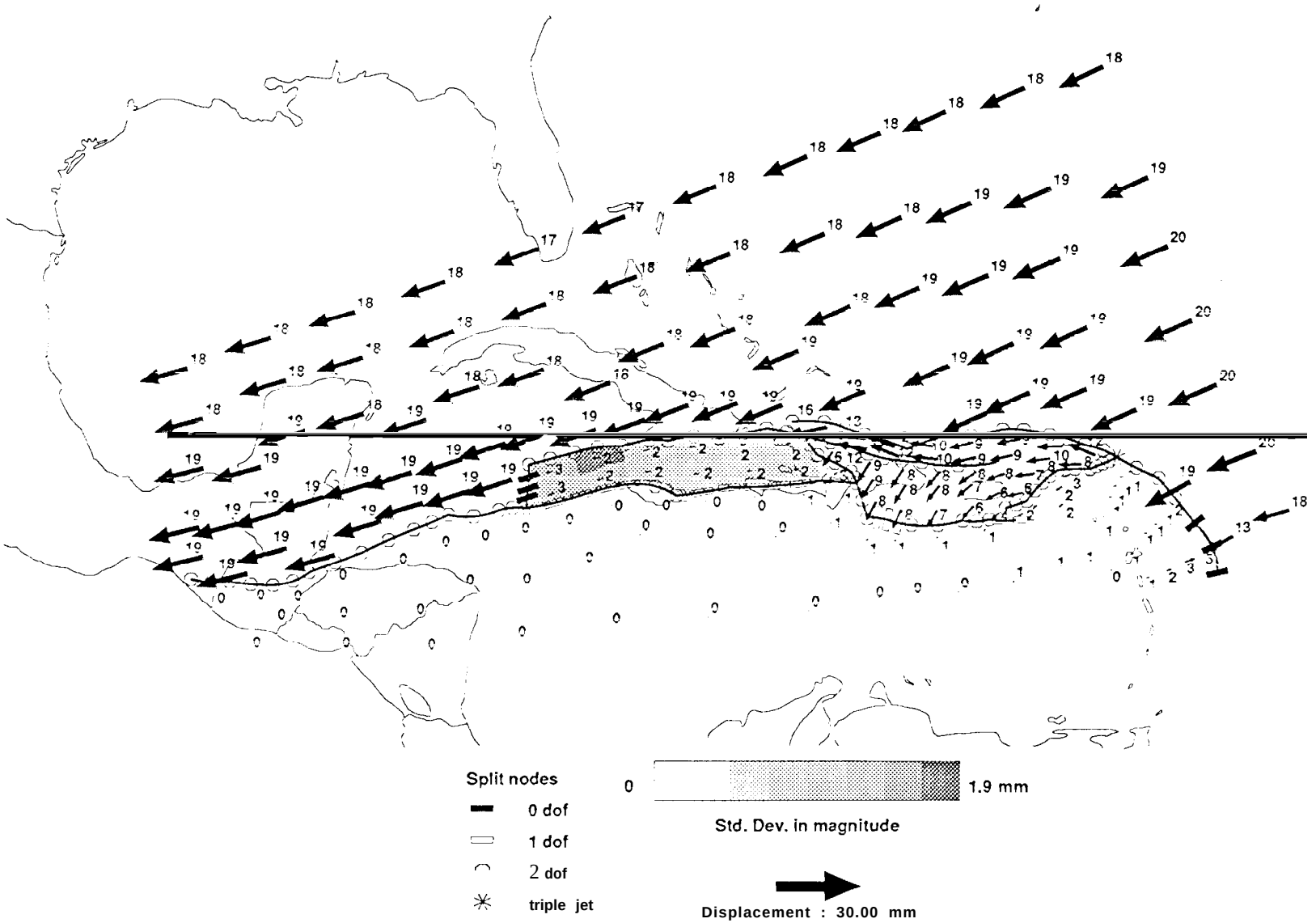
Split nodes
0 dof
1 dof
2 dof
triple jet
0
1.9 mm
Std. Dev. in magnitude
Displacement : 30.00 mm

Figure 4a

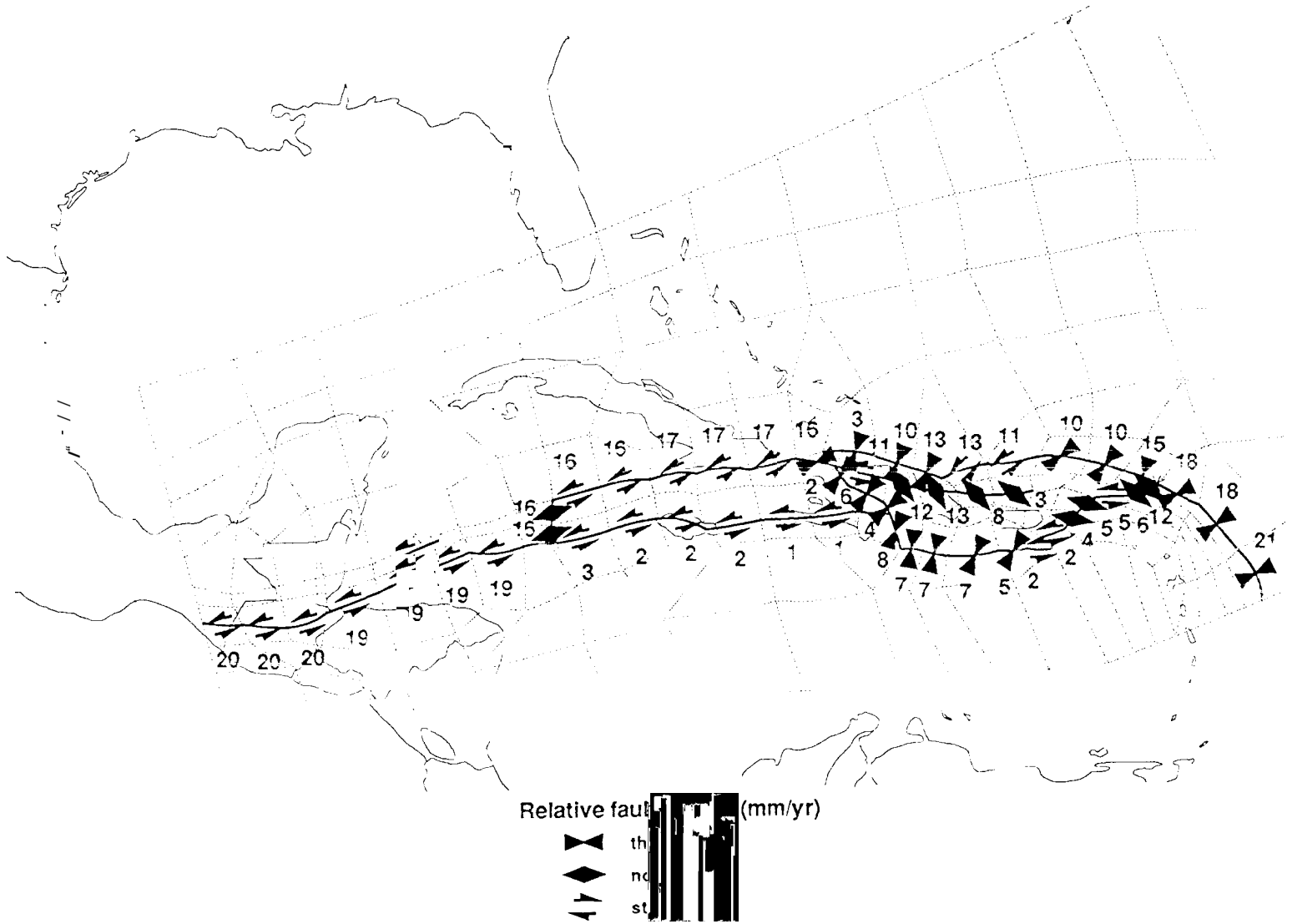

Figure 4b

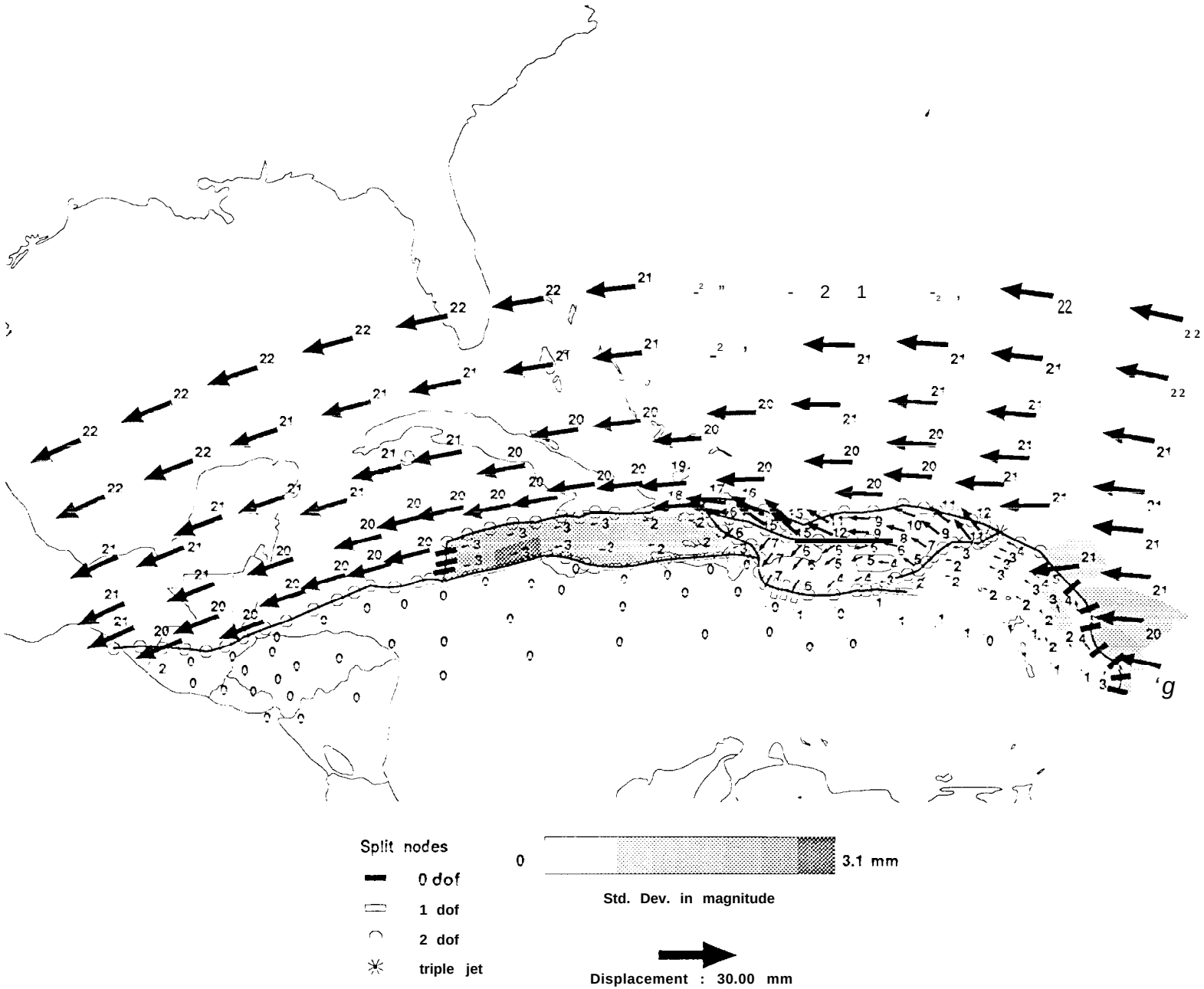
Split nodes
0 dof
1 dof
2 dof
triple jet
0
3.1 mm
Std. Dev. in magnitude
Displacement : 30.00 mm

Figure 5a

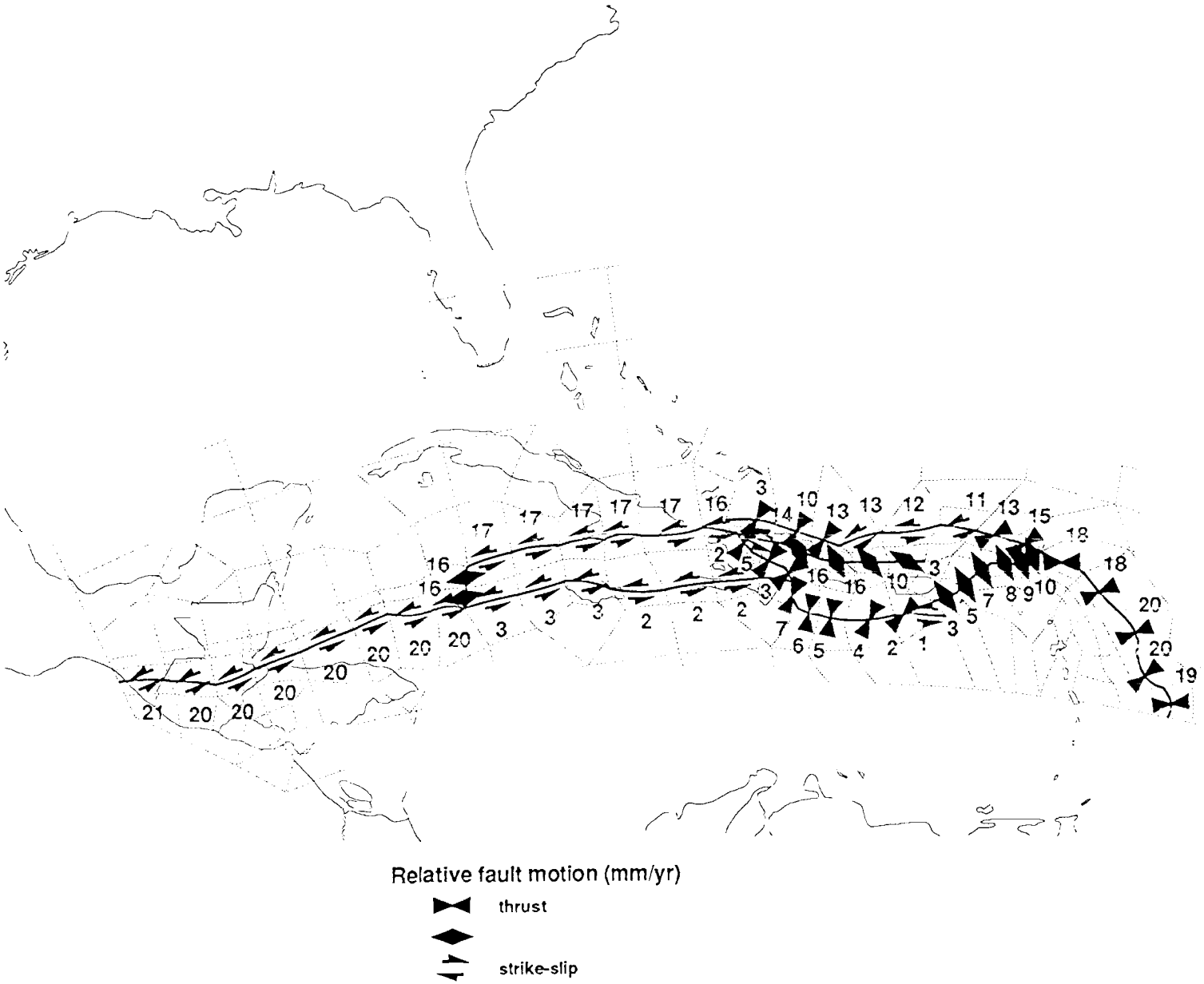

Figure 5b

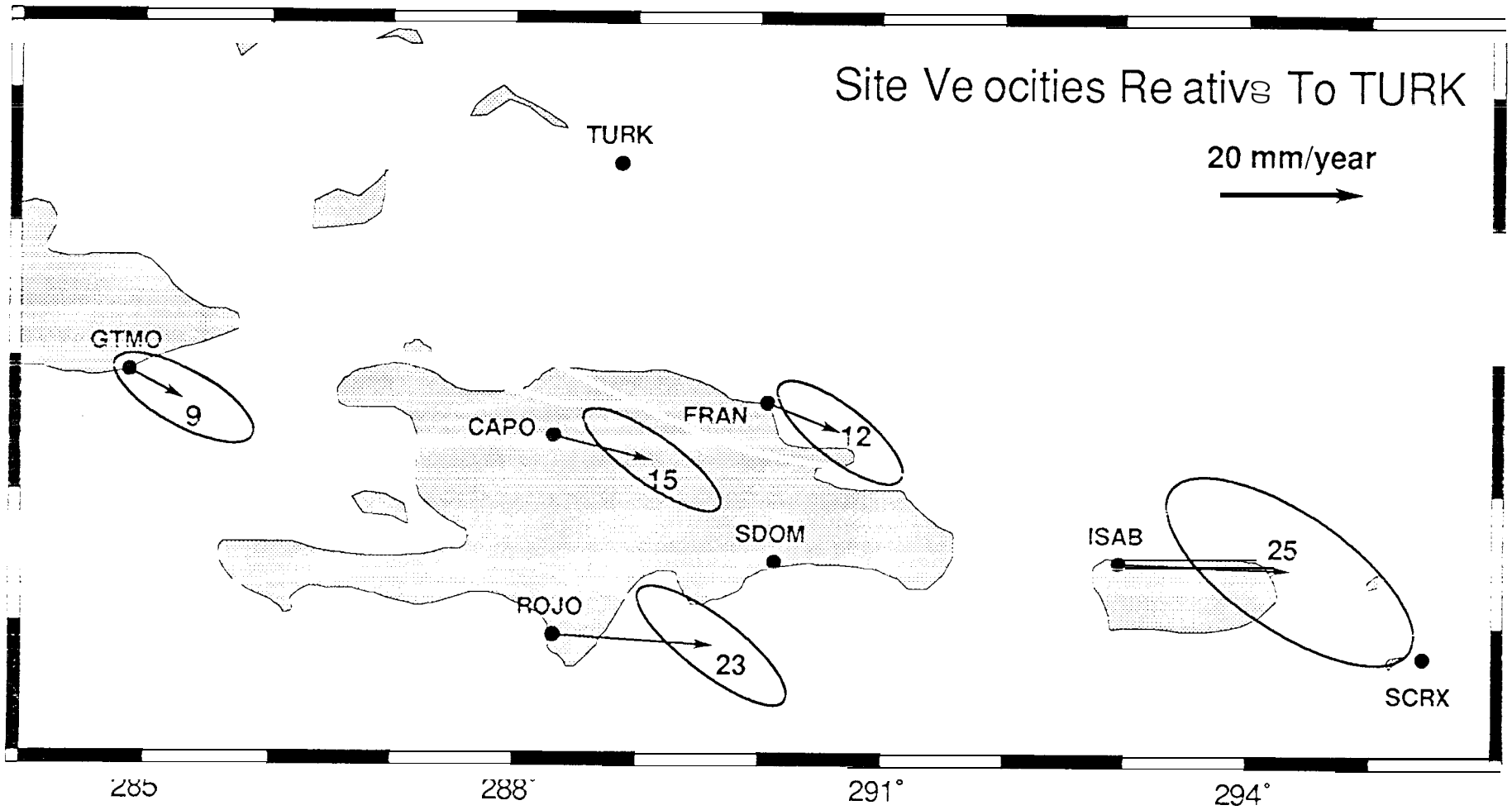
Site Ve ocities Re ativs To TURK
20 mm/year
TURK
GTMO
9
CAPO
15
FRAN
12
SDOM
ROJO
23
ISAB
25
SCRX
285
288°
291°
294°

Figure 6

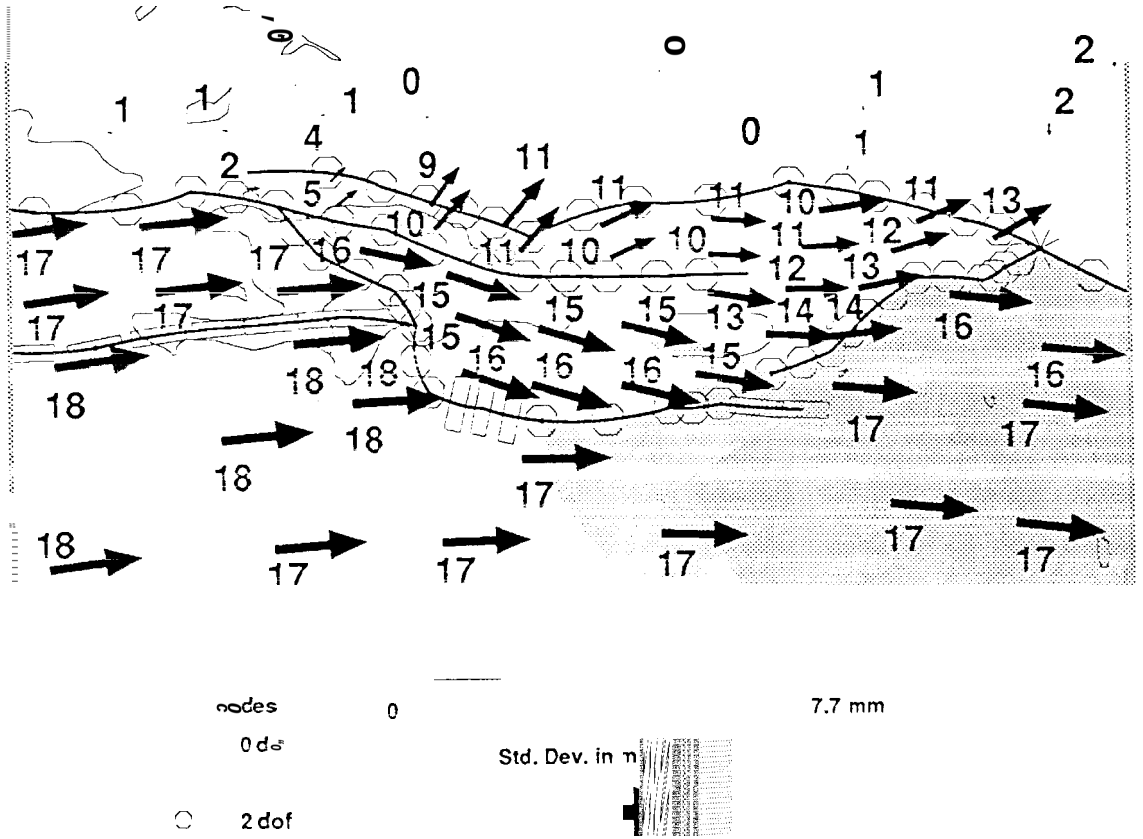

Fig 7

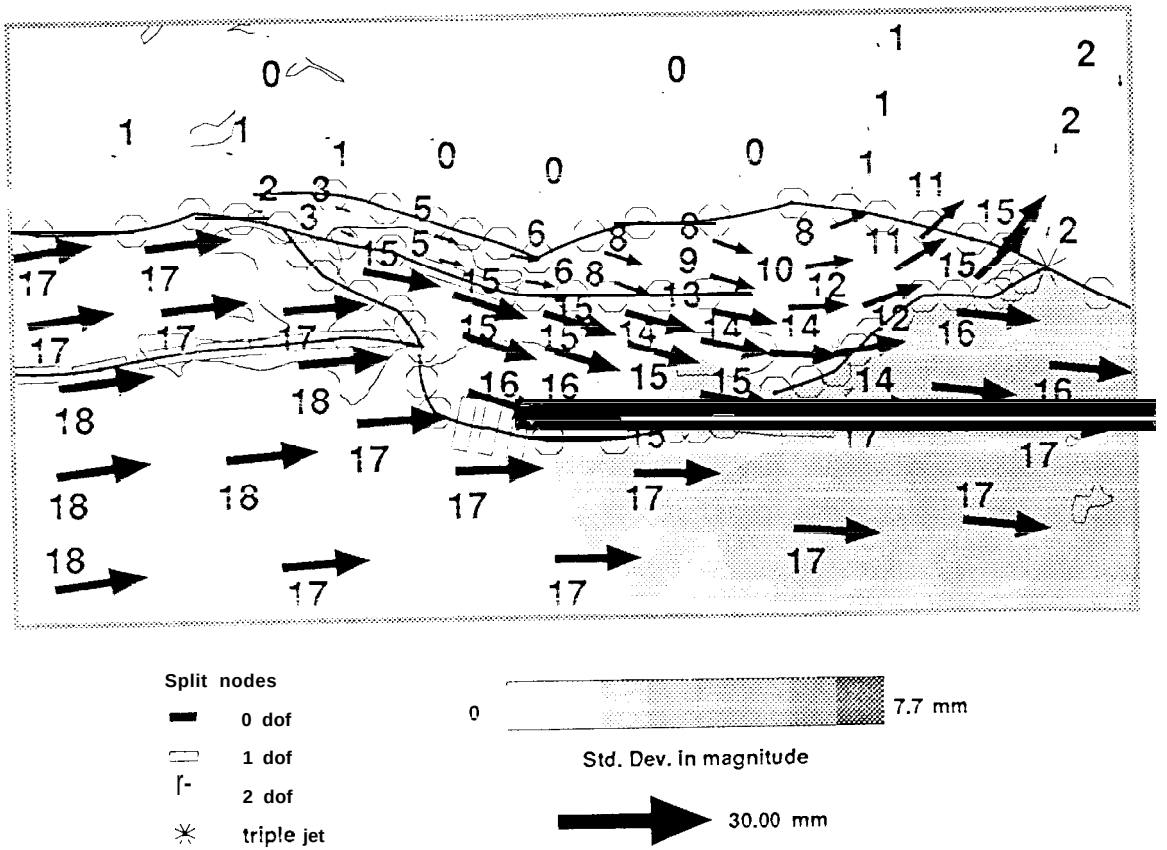
Split nodes
0 dof
1 dof
2 dof
triple jet
0
7.7 mm
Std. Dev. in magnitude
30.00 mm

Figure 8a

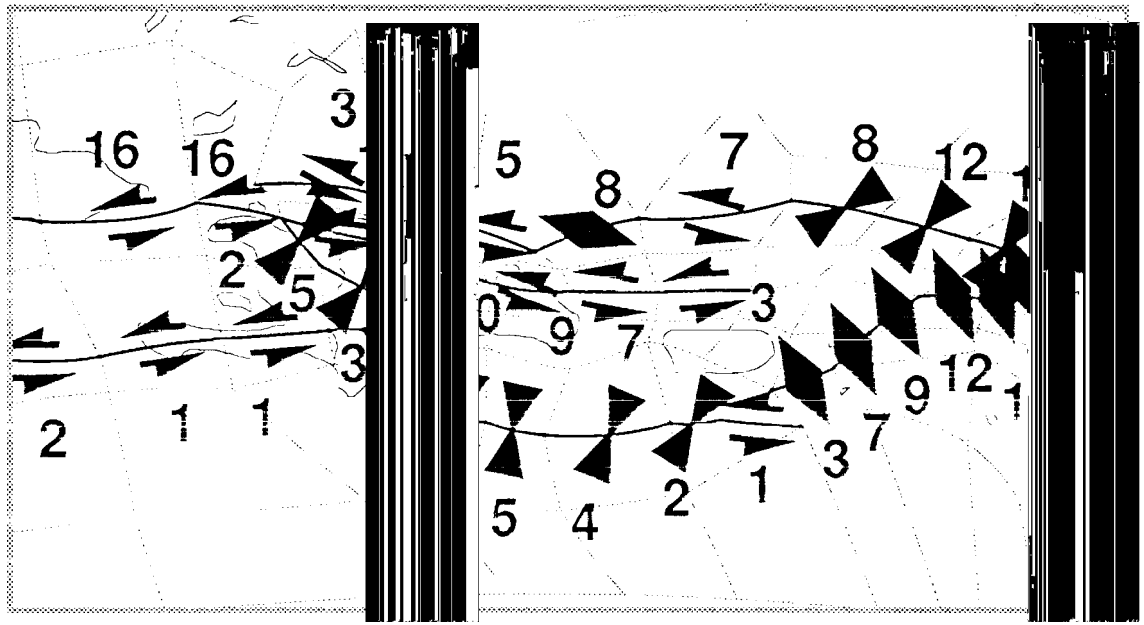

Figu e 8b